Hilbert-Huang Transform and Its Applications in Engineering and Biomedical Signal Analysis

MILAN STORK
Dept. of Applied Electronics and Telecommunications/RICE Faculty of Electrical Engineering,
University of West Bohemia, CZ
stork@kae.zcu.cz

Abstract - Hilbert Huang transform (HHT) is a relatively new method. It seems to be very promising for the different applications in signal processing because it could calculate instantaneous frequency and amplitude which is also important for the biomedical signals. HHT consisting of empirical mode decomposition and Hilbert spectral analysis, is a newly developed adaptive data analysis method, which has been used extensively in biomedical research. Most traditional data processing methodologies are developed under rigorous mathematic rules and we pay a price for this strict adherence to mathematical rigor. Therefore, data processing has never received the deserved aims as data analysis should, and data processing has never fulfilled its full potential - extracting the information hidden in time series. For example, spectral analysis is synonymous with Fourier-based analysis but the Fourier spectra can only give meaningful interpretation to linear and stationary processes and application to data from nonlinear and nonstationary processes is often problematical but the real world is usually nonlinear and non-stationary. In this paper, 3 examples of this approach are presented, which demonstrate the usefulness of the method. The paper will serve also for an introduction of the method for those who want used this approach in industry, biomedical engineering or in other applications.

Key-Words – Amplitude, biomedical, cardiovascular, frequency, Hilbert-Huang transform, modulation, scalogram, wavelet transform

1 Introduction

Hilbert-Huang Transform [1 - 15] is a time-frequency technique consisting of two parts, the Empirical Mode Decomposition (EMD), and the Hilbert Spectral Analysis (HSA). On the first, EMD the signal is decomposed into Implicit Mode Functions (IMF), putting forward the scale characteristics imbedded in the signal. In the second part, the Hilbert transform is applied to the IMF, yielding a time-frequency representation (Hilbert spectrum) for each IMF.

It is important to notice, that the Hilbert transform (HT) can lead to an apparent time-frequency-energy description of a time series; however, this description may not be consistent with physically meaningful definitions of instantaneous frequency and instantaneous amplitude. The EMD can generate components of the time series whose HT can lead to physically meaningful definitions of these two instantaneous quantities, and hence the combination of HT and empirical mode decomposition provides a more physically meaningful time-frequency- energy description of a time series.

An IMF is a function that satisfies two conditions:

- In the whole data set, the number of extrema and the number of zero crossings must either be equal or differ at most by one.
- At any point, the mean value of the envelope defined by the local maxima and the envelope defined by the local minima is zero.

Unfortunately, most time-series do not meet these criteria. At any given time, the data may involve more than one oscillatory mode. This is the reason why the simple Hilbert transform cannot provide the full description of the frequency content in general data. Thus, it is necessary to extract the oscillatory modes IMF from the data, by means of the EMD procedure, which is implemented by an algorithm comprising the following steps:

a) Identify all extrema of $x(t)$

b) Interpolate between minima to obtain the upper envelope $x_U(t)$, and between maxima to obtain the lower envelope $x_L(t)$ (e.g. Fig. 1).

c) Calculate the average envelope $m(t)$

ISBN: 978-1-61804-108-1

$$m(t) = \frac{x_U(t) + x_L(t)}{2} \quad (1)$$

d) Extract the intrinsic oscillatory mode

$$d(t) = x(t) - m(t) \quad (2)$$

e) Iterate on the residual *m(t)*.

In practice, the above procedure has to be refined by first iterating steps a) to d) upon the detail signal *d(t)*, until the latter can be considered as a zero-mean signal according to some stopping criterion.

After a set of iterations (varying within different signals) the zero mean is reached and the first mode of oscillation is them achieved

Interpolation in step b) is made usually using cubic splines, however other interpolation techniques may be applied. The aim of this repeated operation is to eliminate the riding waves and to achieve more symmetrical wave-profile by smoothing the uneven amplitudes. Once this is achieved, the detail is considered as the effective IMF, the corresponding residual is computed and step 5 follows.

Having obtained the IMF's components, it is possible to apply the Hilbert Transform (HT) to each component, to get instantaneous frequency.
The HT of a real signal *x(t)* is defined as

$$H[x(t)] = x * \frac{1}{\pi t} = y \quad (3)$$

or using the convolution definition

$$y(t) = \frac{1}{\pi} P \int_{-\infty}^{\infty} \frac{x(\tau)}{t - \tau} dt \quad (4)$$

where *P* indicates the Cauchy principal value. From *y(t)* it is possible to define the analytical signal $z(t)=x(t)+iy(t)$ or, in polar form, $z(t) = a(t)e^{i\theta(t)}$ in which

$$a(t) = \sqrt{x^2(t) + y^2}, \quad \theta(t) = \arctan\left(\frac{y(t)}{x(t)}\right) \quad (5)$$

Where *a(t)* is instantaneous amplitude and *θ(t)* is instantaneous phase function. Instantaneous frequency *ω(t)* is defined using the instantaneous derivation of phase

$$\omega = \frac{d\theta(t)}{dt} \quad (6)$$

With both amplitude and frequency being a function of time, we can express the amplitude (or energy, the square of amplitude) in terms of a function of time and frequency, *H(ω,t)*. The marginal spectrum can then be defined as

$$h(\omega) = \int_0^T H(\omega, t) dt \quad (7)$$

where [0, *T*] is the temporal domain within which the data is defined. The marginal spectrum represents the accumulated amplitude (energy) over the entire data span in a probabilistic sense and offers a measure of the total amplitude (or energy) contribution from each frequency value, serving as an alternative spectrum expression of the data to the traditional Fourier spectrum.

The signal can be written in the form

$$x(t) = \mathrm{Re}\left[\sum_{j=1}^{n} a_j(t) e^{i\int \omega_j(t)dt}\right] \quad (7)$$

Similarly it is possible to achieve a measure of the energy of the signal with respect to time, if we compute the Instantaneous Energy (*IE*), defined by

$$IE(t) = \int_{\omega} H(\omega, t)^2 d\omega \quad (8)$$

As already reported in the text, the uncritical use of Fourier derived techniques may lead to the extraction of ambiguous information from the data, and in other cases, may lead to failure to extract properties and characteristics of the signal. The use of HHT allows for a decomposition of the signal that resorts to an adaptive set of basis functions. It is therefore possible to use HHT without a predefined choice of parameters.

2 HHT Modulation Signal Example

In this part, the simple example will shown basic properties HHT [16, 17, 18]. An example of amplitude modulation signal is shown in Fig. 1. Input signal, identified maxima and minima, upper and lower envelopes and mean signal are shown. The input signal is

$$y_1 = 0.8 \sin(2\pi t) \cdot \sin\left(2\pi \frac{t}{6}\right) \quad (9)$$

In Fig. 2 (top), the same signal (9) is used with noise

$$y_2 = y_1 + v \quad (10)$$

where *v* is noise (the normal distribution with mean parameter μ = 0 and standard deviation parameter σ = 0.07).

In Fig. 2, the original signal is decomposed into first 7 IMF's components (c_1 to c_7). This first IMF (c_1) should contain the finest scale or the shortest-period oscillation in the signal, which can be extracted from the data by

$$r_1 = y_2(t) - c_1 \qquad (11)$$

The residue, r_1, still contains longer-period variations, as shown in Fig. 2. This residual is then treated as the new data and subjected to the same sifting process as described above to obtain an IMF of lower frequency.

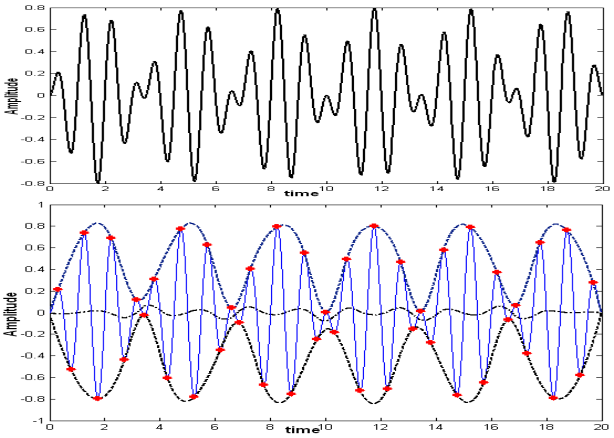

Fig. 1. The input signal (top) and identified maxima and minima (red crosses), upper and lower envelopes (dashed lines) and their mean (dash-dot line, bottom).

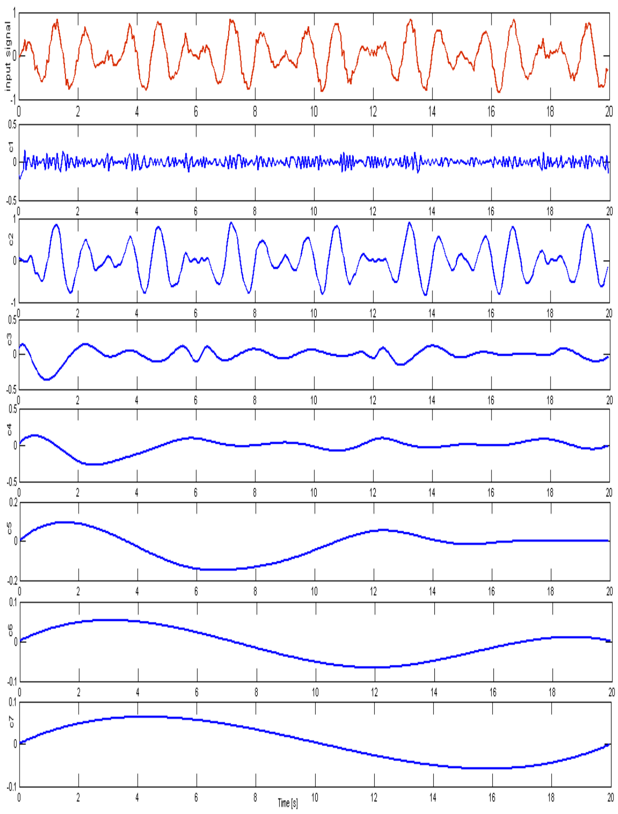

Fig. 2. Example of empirical mode decomposition. Input signal - with noise (top) and $c_1 \ldots c_7$ components, (high to low frequency).

The decomposition process finally stops when the residue, r_n, becomes a monotonic function or a function with only one extremum from which no more IMF can be extracted.

The instantaneous frequencies of signal with noise are shown in Fig. 3.

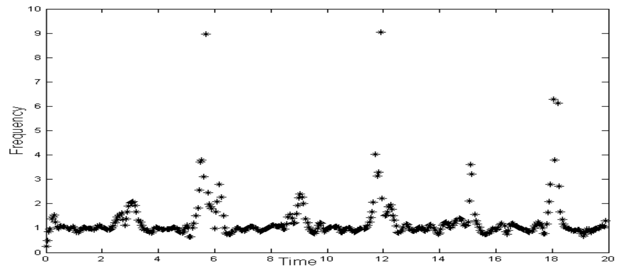

Fig. 3. Instantaneous frequencies of signal with additional noise.

The continuous wavelet analysis to compute the image scalogram of wavelet coefficients is shown in Fig. 4. Scalogram shows energy for each wavelet coefficient.

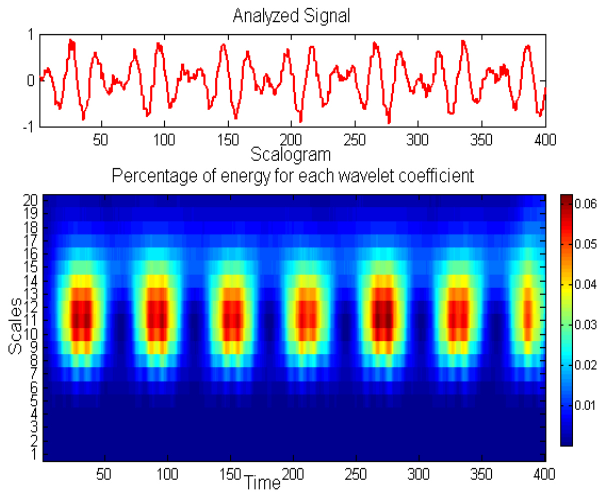

Fig. 4. Time-frequency analysis of modulation – image scalogram.

3 Biomedical Application-1 of HHT

In this part the two examples of biomedical applications of HHT are described. In this, first application, the HHT is used for decompose of electrocardiographic signal (ECG) [19 - 24]. Example of empirical mode decomposition of ECG signal with noise (high frequency components and baseline wandering) is shown in Fig. 5. Input ECG signal is on top and components $c_1 \ldots c_8$ are shown under. In Fig. 6 and 7, the example of instantaneous frequencies of components c_2 and c_3 are displayed.

In Fig. 8, the Time-frequency analysis of ECG signal – contour scalogram is also shown.

ISBN: 978-1-61804-108-1

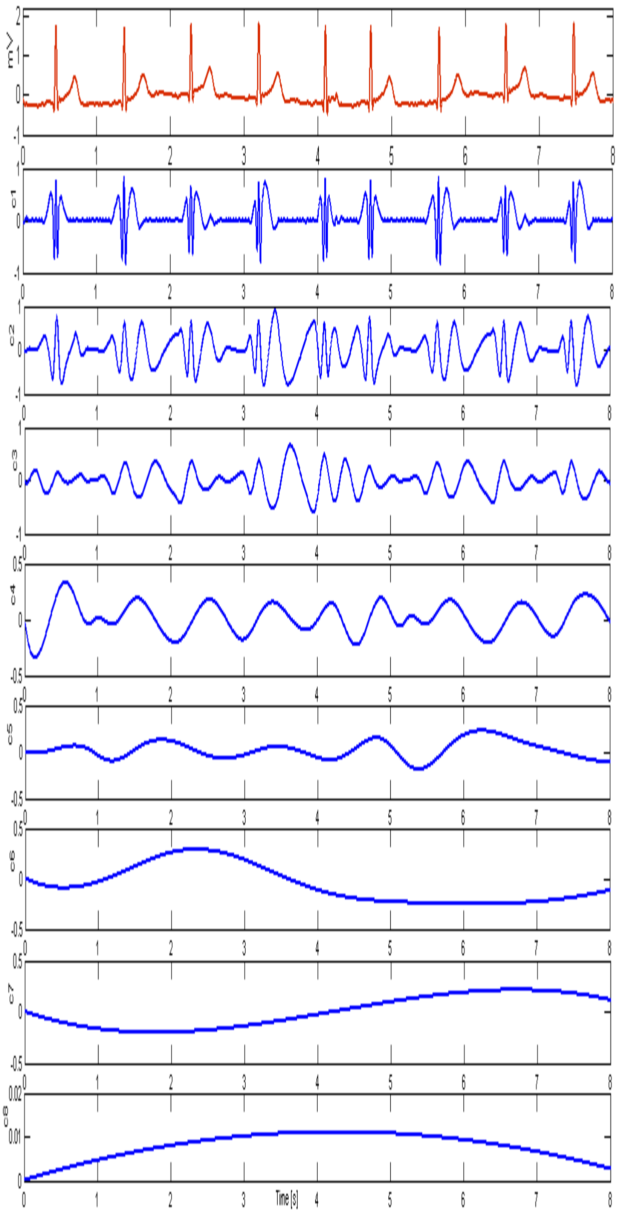

Fig. 5. Example of empirical mode decomposition of ECG signal. Input signal (top) and $c_1 \ldots c_8$ components, (high to low frequency).

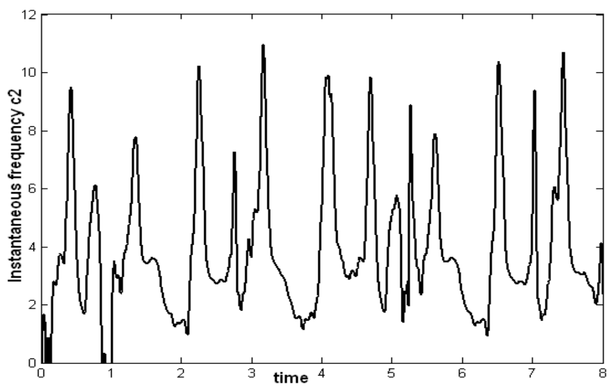

Fig. 6. Instantaneous frequencies of component c_2 of ECG signal.

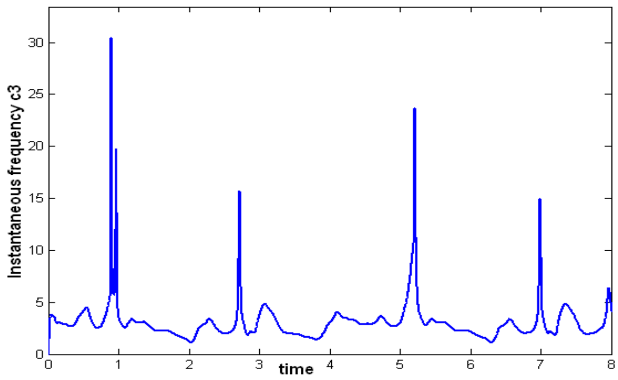

Fig. 7. Instantaneous frequencies of component c_3 of ECG signal.

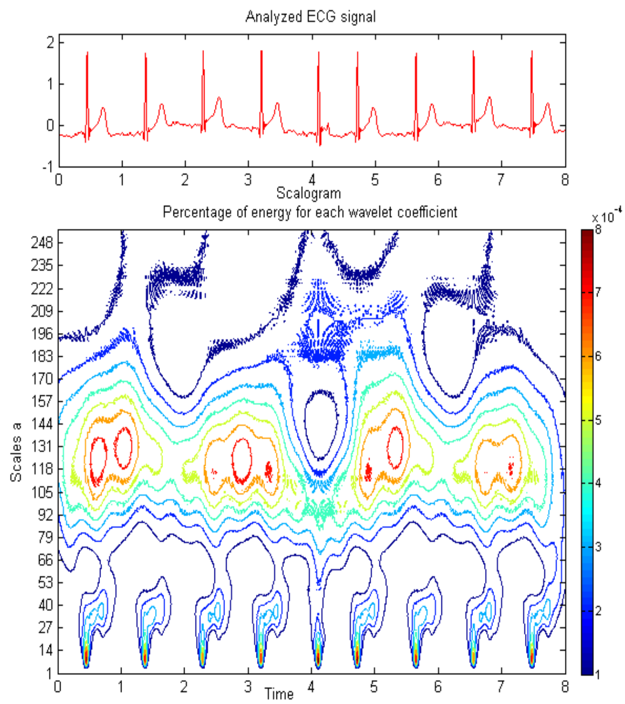

Fig. 8. Time-frequency analysis of ECG signal – contour scalogram.

4 Biomedical Application-2 of HHT

The second biomedical application of HHT is used for balistocardiographic (BCG) signal. The balistocardiography is a noninvasive technique developed for recording and analyzing cardiac vibratory activity as a measure of cardiac contractile performance [25 - 28]. Thus, one may determine the force-response of the cardiovascular system to changes in external stimuli, as well as the autonomous nervous system regulation of the circulation and the activity of the sympathetic and parasympathetic systems. The basic part of the measuring system is a rigid piezoelectric force transducer resting on steel chair. The examined person sits on the seat placed on the transducer and force caused by the cardiovascular activity is a

ISBN: 978-1-61804-108-1

measured (or placing an ultra low-frequency acceleration transducer on the sternum of human subjects).

Usually also heart rate (*HR*) and breathing frequency (*BF*) can be evaluated from BCG signal. It is important to note, that amplitude of measured signal from sensor is sometimes under 1 mV (depend on subject heart activity) and desired frequency spectrum is lower then 30 Hz. The measured signal is corrupted by strong noise, baseline wander, movements of the patient, etc. therefore the analog and digital signal processing (DSP) must be used for signal denoising (e.g. linear analog filter and digital linear and nonlinear filters etc.). The time relations between ECG and BCG and important points of ECG and QSCG signals are shown in Fig. 9.

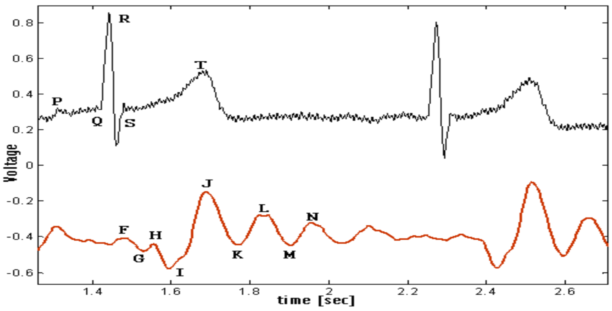

Fig. 9. The important points on ECG (top) and related BCG signal (bottom).

The BCG waveform has been divided into three groups, labeled with letters: pre-injection (FGH), ejection (IJK) and diastolic part of the heart cycle (LMN). The waveform of BCG represents the different phases of the full cardiac cycle. The peek of the H-wave is localized at the end of the contraction phase of the hart and the onset of the rapid expulsion of the blood from the heart into the aorta. The I-wave point reflects the rapid acceleration of blood into the ascending aorta, pulmonary trunk and carotid arteries. The J-wave describes the acceleration of blood in the descending and abdominal aorta, and the deceleration of blood in the ascending aorta. The I-J amplitude reflects the force of contraction of the left ventricle, and the I-J interval reflects its contractility. In normal people, a repeatable pattern of waves occurs with every heartbeat. The example of noised BCG signal and its contour scalogram is shown in Fig. 10.

The discrete BCG signal with noise can be filtered by digital filter or processed by Fourier transform (FT), Wavelet transform (WT) or by Hilbert-Huang transform (HHT).

The scalogram display coefficients on vertical axis and time on the horizontal, and plot energy of signal as a color map (or color contour in contour scalogram). In Fig. 10, the Complex Gaussian wavelet function was used.

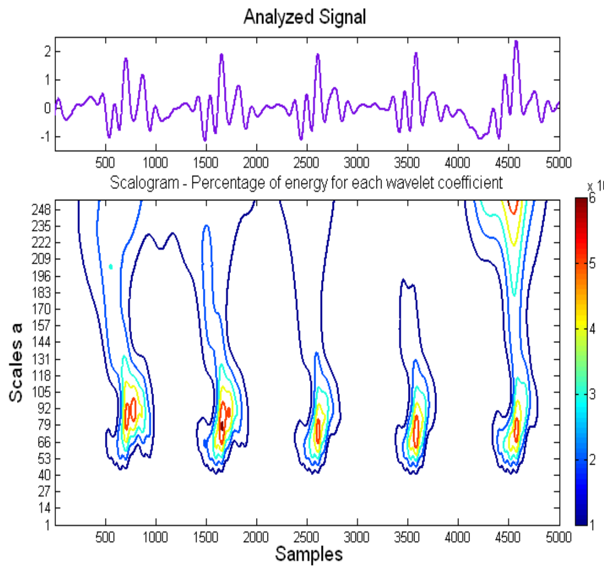

Fig. 10. The example BCG signal (top) and contour scalogram of BCG signal (bottom).

The example of HHT used for QSCG signal is shown in Fig. 11, where the time/frequency of the signal is calculated. In Fig. 12 (top) the input signal is shown and bottom, the HHT decomposition of BCG signal into 10 waves are displayed.

From this decomposition the most important is 4th signal (from the top) which can be directly used for HIJK complex detection of BCG signal (time detection).

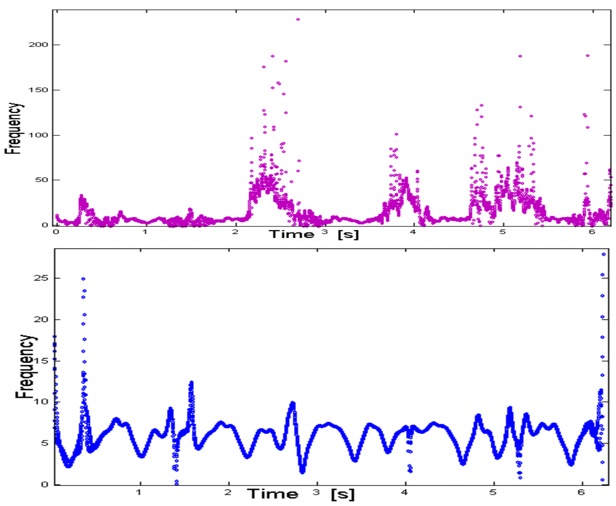

Fig. 11. The HHT - time/frequency of BCG signal. Result for non-filtered signal (top) frequency$\in\langle 0, 250\rangle$ and for filtered signal (bottom) frequency$\in\langle 0, 30\rangle$ (vertical axis).

ISBN: 978-1-61804-108-1

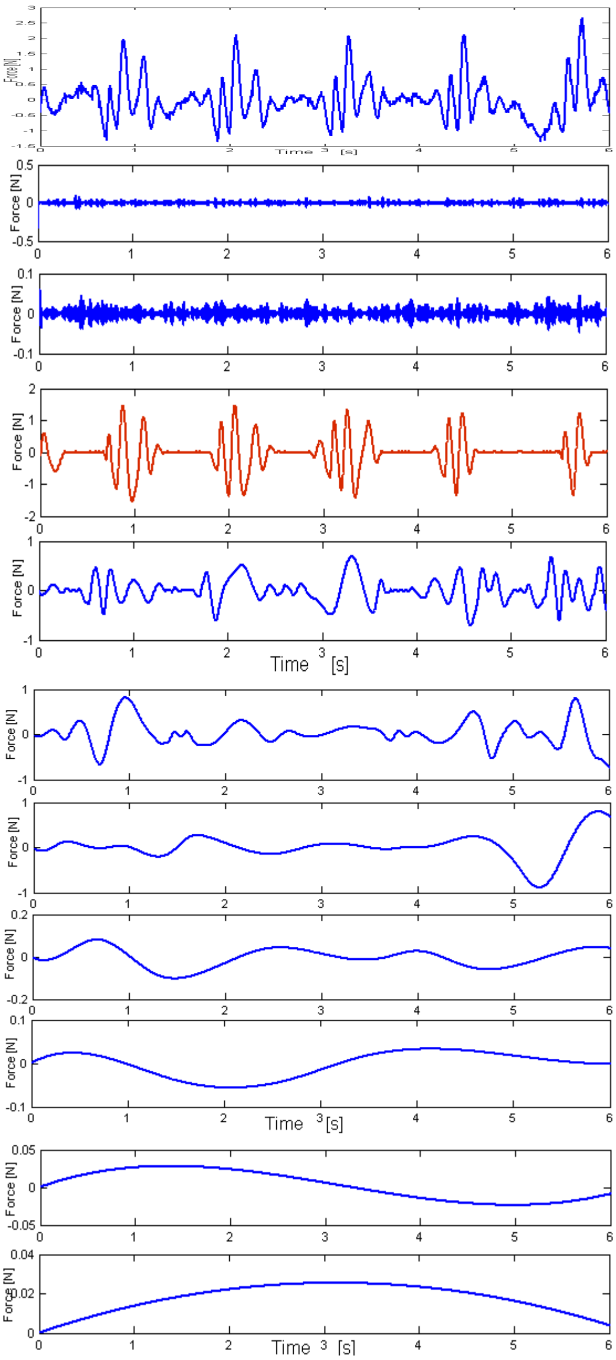

Fig. 12. The input signal (top) and HHT - decomposition of BCG signal (others).

For peaks detection the upper local extrema and lower local extrema is used, see Fig. 13. where a) is input signal, b) lowpass filtered signal, c) filtered signal and upper and lower envelopes, d) input signal with automatic detection of HIJK complex for calculation of systolic force. From this signals, the systolic force F and minute cardiac force MF can be computed according (1) and (2):

$$F = (F_{HI} + F_{IJ} + F_{JK})/3 \qquad [N] \qquad (12)$$

$$MF = F * HR \qquad [N, beats/min] \qquad (13)$$

where HR is heart rate and F_{HI}, F_{IJ}, F_{JK} can be calculated according Fig. 14. The systolic force F represent the force response caused by the heart activity and is expressed in units of force [Newton]. The systolic force is calculated as mean value for fives HIJK complexes. For the total intensity of the heart activity is introduced the minute cardiac force MF which equals the systolic force multiplied by the HR.

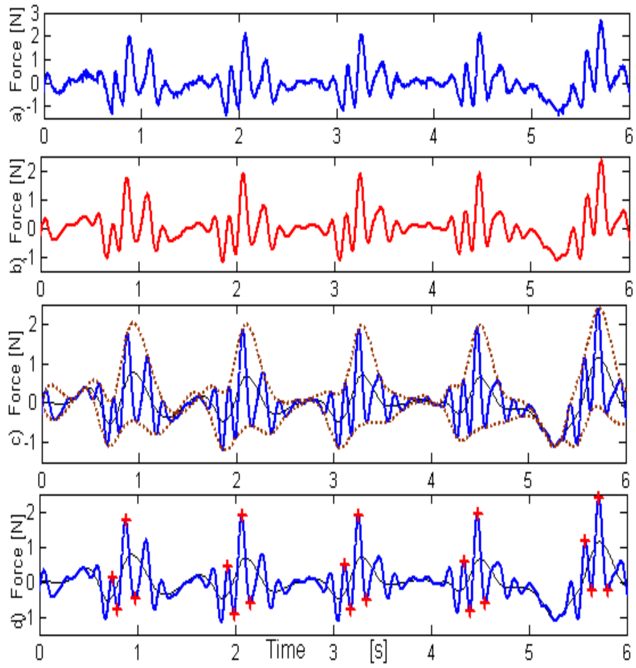

Fig. 13. a) is input signal, b) lowpass filtered signal, c) filtered signal and upper and lower envelopes, d) input signal with automatic detection of HIJK complex.

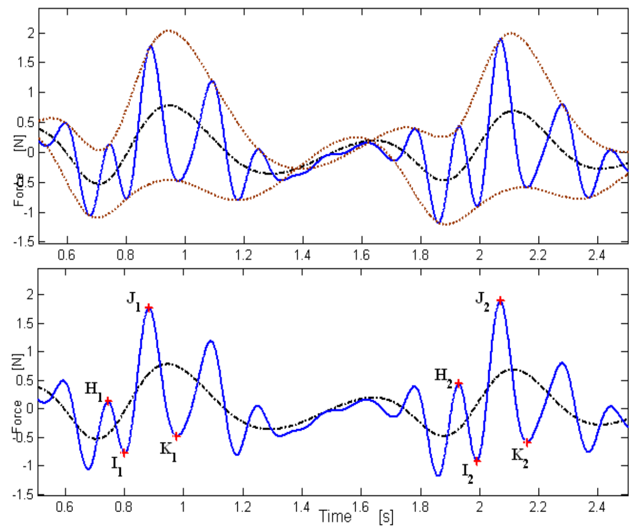

Fig. 14. The zoom of c) and d) of Fig. 13. The HIJK complex of QSCG signal for calculation of systolic force F and minute cardiac force MF. The dash-dot line is average envelope.

ISBN: 978-1-61804-108-1

4 Conclusion

The Hilbert-Huang transform has been shown to be effective for characterizing a wide range of nonstationary signals in terms of elemental components through what has been called the empirical mode decomposition. The HHT has been utilized extensively despite the absence of a serious analytical foundation, as it provides a concise basis for the analysis of strongly nonlinear systems.

In this paper the HHT was shortly described and demonstrated on 3 applications. These applications include simple telecommunication example (amplitude modulation) and 2 examples from biomedical engineering, electrocardiography and balistocardiography.

HHT-based analysis methods are widely applied to biomedical signals, also for electroencephalogram signals, but also for industry and physical signals such as earthquake waves, winds, ocean acoustic signals. It should be noticed that HHT is promising method for signal processing.

ACKNOWLEDGMENT

This research was supported by the European Regional Development Fund and Ministry of Education, Youth and Sports of the Czech Republic under project No. CZ.1.05/2.1.00/03.0094: Regional Innovation Centre for Electrical Engineering (RICE).

References:

[1] N. E. Huang and et al., The empirical mode decomposition and the hilbert spectrum for nonlinear and non-stationary time series analysis, *Proceedings of the Royal Society A: Mathematical, Physical and Engineering Sciences,* 1998.

[2] N. E. Huang, Z. Shen, S. R. Long, M. C. Wu, H. H. Shih, Q. Zheng, N. C. Yen, C. C. Tung , H. H. Liu, The empirical mode decomposition and the Hilbert spectrum for nonlinear and non-stationary time series analysis, *Proc. R. Soc. Lond*. A, 1998, pp. 903-995.

[3] N. Huang and Nii O. Attoh-Okine, *The Hilbert-Huang Transform in Engineering*, CRC Press, 2005.

[4] W. Huang, Z. Shen, N.E. Huang, Y.C. Fung, Engineering analysis of biological variables: An example of blood pressure over 1 day, *Proc. Natl. Acad. Sci. USA*, vol. 95 April 1998, pp. 4816-4821

[5] N. E. Huang, Computer implemented empirical mode decomposition apparatus, method and article of manufacture for two-dimensional signals, *Patent 6311130, U.S. Patent and Trademark Off.*, Washington, D. C. 2001.

[6] N. E. Huang, Empirical mode decomposition for analyzing acoustical signals, *Patent 6862558, U.S. Patent and Trademark Off.,* Washington, D. C. 2005.

[7] N. E. Huang, Computing instantaneous frequency by normalizing Hilbert transform, *Patent 6901353, U.S. Patent and Trademark Off.*, Washington, D. C. 2005.

[8] N. E. Huang, et al., A confidence limit for the empirical mode decomposition and Hilbert spectral analysis. *Proc. R. Soc. London*, 2003, pp. 2317–2345.

[9] N. E. Huang and Z. Wu, A Review on Hilbert-Huang Transform: Method and its Applications to Geophysical Studies, *Reviews of Geophysics*, 46, RG2006, 2008, pp. 21-26/

[10] R. Liu, Empirical mode decomposition: A useful technique for neuroscience?, 2002.

[11] L. Cohen, *Time Frequency Analysis: Theory and Applications*, 320 pp., Prentice-Hall, Englewood Cliffs, N. J., 1995.

[12] C. Damerval, S. Meignen, and V. Perrier, A fast algorithm for bidimensional EMD, *IEEE Signal Process. Lett*., 12, 2005, pp. 701–704, doi:10.1109/LSP.2005.855548.

[13] M, Datig and T. Schlurmann, Performance and limitations of the Hilbert-Huang transformation with an application to irregular water waves, *Ocean Eng*., 31, 2004, pp. 1783–1834, doi:10.1016/j.oceaneng.2004.03.007.

[14] P. Flandrin, G. Rilling, and P. Goncalves, Empirical mode decomposition as a filter bank, *IEEE Signal Process. Lett.*, 11, 2004, pp. 112–114, doi:10.1109/LSP.2003.821662.

[15] N.-C. Yen, C. C. Tung, and H. H. Liu, The empirical mode decomposition and the Hilbert spectrum for nonlinear and nonstationary time series analysis, *Proc. R. Soc. London, Ser. A*, 454, 1998, pp. 903–993.

[16] D. S. Laila, M. Larsson, B. C. Pal, and P. Korba, Nonlinear damping computation and envelope detection using Hilbert transform and its application to power systems wide area monitoring, *IEEE Power and Energy Soc. General Meeting*, 2009

[17] D. S. Laila, A. R. Messina, and B. C. Pal, Variants of Hilbert-Huang transform with applications to power systems oscillatory dynamics, *Analysis of Nonlinear and Non-stationary Inter-area Oscillations: A Time-*

Frequency Perspective, Ed. New York: Springer, 2009.

[18] N. Senroy, S. Suryanarayanan, and P. F. Ribeiro, An improved Hilbert-Huang method for analysis of time-varying waveforms in power quality, *IEEE Trans. Power Syst*., vol. 22, no. 4, pp. 1843–1850, Nov. 2007.

[19] Y. Huang, D. Erdogmus, K. E. Hild , M. Pavel, and S. Mathan, *Mixed effects models for single-trial ERP detection in noninvasive brain computer interface design*, Recent Advances in Biomedical Signal Processing, Bentham Science Publishers, July 2010.

[20] Y. Huang, K. Englehart, B. Hudgins, and A.D.C Chan, A Gaussian mixture model based classification scheme for myoelectric control of powered upper limb prostheses, *IEEE Transactions on Biomedical Engineering*, vol. 52, no. 11, pp. 1801-1811, Nov. 2005.

[21] Y. Huang, D. Erdogmus, M. Pavel, K. E. Hild and S. Mathan, A hybrid generative/discriminative method for EEG evoked potential detection, *The 4th Intl. IEEE EMBS Conf. on Neural Engineering*, Turkey, 2009.

[22] Y. Huang, D. Erdogmus, M. Pavel, S. Mathan, Mixed effects models for EEG evoked response detection, *IEEE Intl. Workshop on MLSP*, Cancun, Mexico, 2008.

[23] Chin-Feng Lin, and Jin-De Zhu, HHT-Based Time-Frequency Analysis Method for Biomedical Signal Applications, *Recent Advances in Circuits, Systems, Signal and Telecommunications, 5th WSEAS International Conference on CIRCUITS, SYSTEMS, SIGNAL and TELECOMMUNICATIONS (CISST '11)*, Mexico, 2011, pp. 2135-2146

[24] M. Stork, J. Novak, V. Zeman, Noninvasive cardiac output estimation based on oxygen consumption during stress test, *Proceedings of the 14th WSEAS international conference on Systems : part of the 14th WSEAS CSCC multiconference* - Volume I, ISBN: 978-960-474-199-1, 2010, pp. 159-164.

[25] M. Stork, D. Mayer, J. Hrusak, High resolution analog-digital converter and digital polynomial filter applications, *5th WSEAS International Conference on Applications of Electrical Engineering*, Prague, Czech Republic, March 12-14, 2006, pp. 69-74.

[26] Z. Trefny, M. Stork, M. Trefny, "Electronic Device for Seismocardiography, Noninvasive Examination and Signal Evaluation," *Biostec – Second International Point Conference on Biomedical Engineering Systems and Technologies*, 14-17 January, Porto, Portugal, ISBN: 978-989-8111- 64-7, 2009.

[27] M. Stork, Z. Trefny, Quantitative Seismocardiography System With Separate QRS Detection, *20-th International EURASIP Conference BIOSIGNAL, Analysis of Biomedical Signals and Images*; vol. 20, pp. 61-68, 2010.

[28] M. Stork, Z. Trefny, New seismocardiographic measuring system with separate QRS detection, *Proceedings of the 14th WSEAS international conference on Systems: part of the 14th WSEAS CSCC multiconference - Volume I*, ISBN: 978-960-474-199-1, 2010, pp. 176-180.